SAND2008-7394P

Solid State Lighting
Budget Period Continuation
Topical Report

November 4, 2008

Innovative Strain-Engineered InGaN Materials for High-Efficiency Deep-Green Light Emission

Work Performed Under Agreement:
M6642865

Submitted By:
Sandia National Laboratories[1]
Mail Stop 1086
Albuquerque, NM 87185

Principal Investigators:
Michael E. Coltrin[2] and Stephen R. Lee[3]

Submitted To:

U. S. Department of Energy
National Energy Technology Laboratory
Project Officer: Brian Dotson
E-Mail: Brian.Dotson@netl.doe.gov

[1] Sandia is a multiprogram laboratory operated by Sandia Corporation, for the United States Department of Energy's National Nuclear Security Administration under contract DE-AC04-94AL8500.

[2] Phone: (505) 844-7843; Fax: (505) 844-3211; E-mail: mecoltr@sandia.gov

[3] Phone: (505) 844-7307; Fax: (505) 844-3211; E-mail: srlee@sandia.gov

Table of Contents

1. Project Objective....3
2. Expected Benefits....3
3. Funding and Costing Profile....5
4. Future Budget Periods Overview....5
5. Description of Work Performed on Tasks....6
6. Status of Milestones....15
7. Cooper Stage-Gate Progress....19
8. Deliverables....19
9. Final Product / Commercialization....19

1. Project Objective

The goal of this project is to develop high-efficiency deep-green (≥ 545 nm) light emitters based on strain-engineered InGaN materials. This objective is crucial for success of the multi-chip approach to energy-efficient solid-state lighting, which combines output from red, green, and blue (RGB) LEDs to produce white light. We will improve internal quantum efficiency (IQE) by developing thick, strain-relaxed InGaN templates for growth of deep-green active regions. These novel templates will enable active-region quantum wells (QWs) with much lower strain than is currently possible using GaN templates. Reduced strain lowers the piezoelectric field in the QWs, resulting in improved light-emission efficiency. Since strain fundamentally limits indium incorporation during InGaN growth, reduced strain also raises the attainable indium composition at a given growth temperature, making longer emission wavelengths possible without suffering from enhanced defect formation at lower growth temperatures. We will fabricate and test p-n junction structures to quantify the IQE of these improved materials, with a final project goal of demonstrating an IQE at 545 nm that is at least 2.5X greater than that of current-state-of-the-art deep-green LEDs.

2. Expected Benefits

The stated mission for DOE's Lighting Research and Development Program is to increase end-use efficiency through new lighting technologies that have the potential to conserve 50% of electric lighting consumption by 2025. Meeting this goal depends upon the success of solid-state white lighting for general illumination purposes.

Successful development of efficient green LEDs is crucial in the multi-chip approach to producing energy-efficient white luminaires without employing phosphors. This approach combines the output of separate red, blue, and green LEDs to produce white light. However, the luminescence efficiency of current state-of-the-art green LEDs is far less than for blue (GaN) and red (AlGaInP) LEDs. This is a direct result of the low luminescence efficiency of high InN-content InGaN QWs. This problem is compounded because the green portion of the visible spectrum is the region in which the human eye is most sensitive. An increase in luminescence efficiency in this emission region would be a great advance for energy-efficient solid-state lighting.

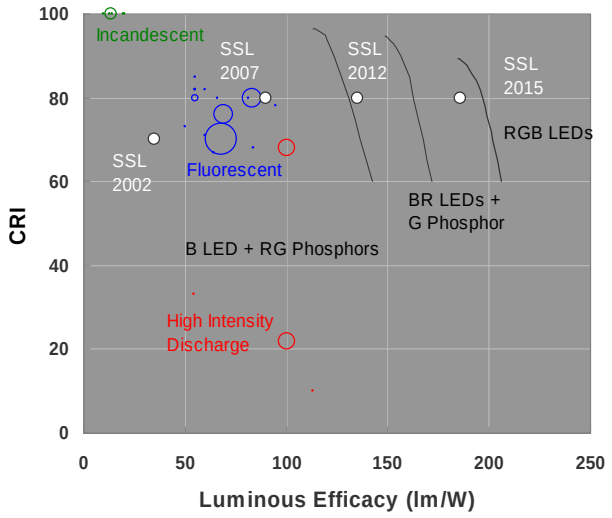

Figure 1. Trade-offs between CRI and luminous efficacy for different LED / phosphor schemes.

Our project centers on improving InGaN materials to improve the IQE of green light emission. The areas of high-efficiency materials research and green wavelengths are at the top of priorities identified during the Solid-State Lighting Program Planning Workshop held on February 3-4, 2005,

in San Diego, CA. *Specifically, in the ranking of importance, task 1.1.2 "High - efficiency semiconductor materials" received more votes by workshop participants than any other inorganic core-research topical area.*

The EERE SSL Multi-Year Plan targets for 2015 are a luminous efficacy of 186 lm/W with a CRI of 70-80. For all of the approaches to solid-state white lighting (RGB LEDs; RB LEDs + G Phosphor; B LED + RG Phosphors), there is a trade-off between CRI and luminous efficacy. For example, concentrating most of the light output (lumens) in the green, where the human eye is most sensitive, would increase the luminous efficacy, but at the same time would decrease the CRI. Conversely, expanding the output to fill the entire visible spectrum would increase the CRI, but your eye would also be seeing colors to which it is not very sensitive, so luminous efficacy would decrease.

This trade-off can be made quantitative using a luminous-efficacy-CRI simulator, which, for a given CRI, solves for those wavelengths that maximize the luminous efficacy. For the curves in Figure 1, we have used a simulator developed by Yoshi Ohno at National Institute of Standards and Technology (NIST). For the characteristics of the white light, we assume a constant color temperature of 4,000K, with no allowed deviation from Planckian white. For the characteristics of the LEDs and phosphors we assumed: 50% EQE and 20 nm linewidths for the LEDs and 90% efficiency and 80 nm linewidths for the phosphors. The Stokes shift energy loss in the phosphors was also taken into account.

One can see that of the three approaches to white light, the one most commonly used today, based on a blue LED and red, green phosphors, has the least desirable "envelope." At a CRI of 80, which is perhaps the minimum CRI necessary to compete with traditional lighting, this approach is limited to a luminous efficacy of 131 lm/W. An intermediate approach, based on blue and red LEDs with a green phosphor, which one might use if an efficient green LED is not developed, can achieve a luminous efficacy of 163 lm/W. The best approach is the red, green, blue LED approach, which can achieve a luminous efficacy of 198 lm/W.

For a given CRI, the RGB LED approach has a roughly 20-50% higher luminous efficacy than the blue + phosphor approaches. However, *the major hurdle for success of the three-color scheme is the availability of an efficient LED in the green.*

The needed wavelengths for the RGB LED approach to white light with a CRI of 80 and a luminous efficacy of 198 lm/W are: 458 nm, 540 nm and 604 nm. As the wavelength of the green LED is further shortened from the peak of the human eye sensitivity curve (555 nm), the best-attainable luminous efficacy at the same CRI of 80 also decreases; the optimal wavelength for the blue and red LEDs would also be shortened, to maintain CRI. If the green wavelength were 530 nm (along with 455 nm blue and 599 nm red), the best luminous efficacy becomes 196 lm/W; at 520 nm green (along with 441 nm blue and 597 nm red) it becomes 186 lm/W; and at 510 nm green (along with 432 nm blue and 593 nm red) it becomes 172 lm/W. The decrease in luminous efficacy is of course undesirable; the shortening of the red LED wavelength is also undesirable because red LED efficiency also drops strongly with wavelength. Hence, *improvements in the InGaN epitaxial growth needed to achieve deep-green emission are crucial for meeting SSL efficiency goals.*

3. Funding and Costing Profile

Table I shows, by Budget Period, the amount of government funding going to Sandia National Laboratories. Since Sandia National Laboratories is a prime contactor to DOE there is no cost sharing in this project.

Table I. Project funding profile.

	BP#1		BP#2		BP#3		Total	
	Gov. Funding	Cost Share	Gov. Funding	Cost Share	Gov. Funding	Cost Share	Gov. Funding	Cost Share
Sandia National Labs	$599,000	$0	$599,000	$0	$599,000	$0	$1,797,000	$0
Total:	$599,000	$0	$599,000	$0	$599,000	$0	$1,797,000	$0

4. Future Budget Periods Overview

A total of five Tasks, spanning three Budget Periods, comprise the project:

Budget Period 1 ran from 7/1/06 to 9/30/07; Budget Period 2, which was just completed, ran from 10/1/07 to 9/30/08; upcoming Budget Period 3 will run from 10/1/08 to 9/30/09.

Task 1 is development of planar heteroepitaxy of strain-relaxed InGaN (on GaN / sapphire) templates using metal-organic chemical vapor deposition (MOCVD). This effort spans the first 27 months of the project.

Task 2 investigates the utility of epitaxial lateral overgrowth (ELO) for growth of low dislocation density, strain-relaxed InGaN. In the first 12 months we conducted survey experiments to characterize the process. The process will be optimized for growth of strain-relaxed InGaN (with increasing In-composition) in Budget Periods 2 and 3. In July of 2007, this task was redirected to sub-micron, nanopatterned growth strategies that enable InGaN materials behavior not attainable using micron-scale patterning.

Task 3 is the growth of optimized InGaN quantum-well active regions on the strain-relaxed InGaN templates developed in Tasks 1 and 2. Target In-compositions and emission wavelengths increase each Budget Period as the project proceeds.

Task 4 is development of a thermally compatible (that is, low-temperature) process for growing p-doped InGaN. This task began in the second Budget Period, and runs through the end of the project.

Task 5 is evaluation of the internal quantum efficiency of our deep-green emitters produced by the strain-engineering tasks above. This task was to begin in the second Budget Period and runs through the end of the project. However, it has been delayed due to the difficulty encountered in attaining sufficient material quality in Tasks 1 and 2 to devote resources to making device structures.

Work planned for Budget Period 3:

In Budget Period 3, our work will mainly focus on Task 2, Task 3, and Task 5. Task 2 work on nanopatterned InGaN will seek to reduce the threading-dislocation density of our strain-relaxed InGaN templates while maintaining the good surface morphology and high degree of strain relaxation already attained using some of our other growth strategies. Task 4 work will further optimize the growth of InGaN quantum-well active regions on top of the improved strain-relaxed InGaN templates produced under Task 2. If Task 2 and Task 4 prove successful, Task 5 work will then evaluate the IQE of the resulting light-emitting active regions. We will perform initial evaluations of IQE using room-temperature and temperature-dependent photoluminescence. If these results are promising, we will proceed to final tests of actual electroluminescent devices (i.e., LEDs) that incorporate our strained-relaxed InGaN templates and associated active regions.

5. Description of Work Performed on Tasks

In this section, we review project work performed during our 3-month extension to Budget Period 1 and during Budget Period 2. Further details appear in our monthly reports.

Task 1 / Approach 1: Growth of InGaN using AlN interlayers

This approach was examined during Budget Period 1; minimal further experiments were conducted during the present reporting period.

Task 1 / Approach 2: Improvement of strain-relaxed-InGaN surface morphology using GaN planarization layers

We grew a series of strain-relaxed InGaN/GaN superlattices containing thin, periodic GaN layers intended to promote surface planarity in the relaxed InGaN as it grows. To promote planarization, these GaN layers must be grown at a much higher temperature than the surrounding InGaN. However, the tendency of the InGaN to decompose at higher temperatures limits the allowable temperature for the GaN growth. We intentionally varied the growth temperature of the GaN layers in order to determine the lowest growth temperature where they remain effective.

The GaN planarization layers are quite effective at 950 ºC growth temperature and yield an rms surface roughness as low as 0.65 nm for InGaN/GaN superlattices. As growth temperature is decreased to 920 ºC, there is a modest increase in roughness to 1.2 nm; further decreases in temperature produce an exponential rise in roughness. The surface is characterized by planar, overlapping platelets at 950 ºC, and as temperature is decreased, the surface develops a network of convoluted channels. At the lowest temperature examined, 906 ºC, the channeled surface converted to a denser array of fully separated mesas that gave the surface a pebble-like appearance.

The overall temperature dependence suggests that ~ 920 ºC is the lowest GaN growth temperature capable of producing a useful degree of planarization during InGaN growth.

The maximum $In_xGa_{1-x}N$ composition compatible with use of GaN planarization layers grown at 920 º is limited to about x=0.12 (± 0.02); higher-composition InGaN alloys noticeably decompose during growth of GaN planarization layers.

Task 1 / Approach 3: Growth on low-threading-density GaN templates

The goal of this approach is to eliminate both the formation of v-defects and associated strain-relaxation modes by reducing the GaN threading dislocations that are the nucleation sites for v-defect formation. In the absence of v-defects and associated threads, previous work done at Arizona State University (ASU) [S. Srinivasan, *et al.,* Appl. Phys. Lett. **83**, 5187 (2003)] has suggested that InGaN grown on GaN will shift to a more favorable strain-relaxation mode characterized by pure misfit-dislocation glide. Our work in this area tests this hypothesis and attempts to put it to use for producing strain-relaxed InGaN templates suitable for subsequent active-region growth.

Optimization of Cathodoluminescence-Imaging Capabilities:

In our Budget Period 1 experiments, it was unclear from XRD experiments whether or not the strain relaxation produced by this approach proceeded by misfit glide as suggested by Srinivasan, *et al*. Because routine imaging of the these misfits by transmission electron microscopy (TEM) is very laborious and time consuming, we decided to develop nondestructive cathodoluminescence (CL) imaging as a more efficient alternative method for detecting dislocation formation in our InGaN heterostructures.

To increase the band-edge light emission needed for successful CL imaging, we performed a detailed study of the effects of Si-doping concentration, InGaN-alloy composition, and V/III ratio on the InGaN luminescence intensity. Resulting room-temperature photoluminescence (PL) intensity (which served as a test proxy for CL-image contrast) showed a very strong dependence on Si-doping concentration for doping levels less than ~$3x10^{18}$ /cm^3. Above this doping level, relatively constant PL intensity levels were reached, at least for $x \leq 0.15$. The overall InGaN luminescence intensity varied by a remarkable factor, up to ~1230X, for $In_xGa_{1-x}N$ compositions in the range x~0.07 to 0.18 and for Si-doping concentrations ranging from ~$1x10^{17}$ up to ~$1.5x10^{19}$ cm^{-3}. These wide variations demonstrate the need for proper optimization of doping levels and growth conditions in order to obtain high-contrast CL images. Based on these results, subsequent growths of thick InGaN were Si doped at $3x10^{18}$ /cm^3 in order to facilitate post-growth CL imaging of dislocations.

Inducing Long-Range Misfit-Dislocation Glide:

In an attempt to induce long-range misfit-dislocation glide, we grew several different sets of thick InGaN samples on low-threading-density GaN templates. Three types of low-threading-density GaN templates were used in these studies: (i) ELO-type, (ii) ULD-type (basically, ELO accomplished using a SiN_x "auto-masking" technique), and (iii) bulk GaN grown by HVPE. The threading densities for these templates ranged from ~$5x10^6$ to ~$1x10^8$ cm^{-2}, which is significantly less than that for our standard GaN templates on sapphire, ~$5x10^8$ cm^{-2}. All experiments were conducted using simultaneously grown 3-wafer sets enabled by the multi-wafer capability of our MOCVD reactor. Each set of wafers made use of two of the three types of specialty-GaN templates described above; the third wafer was

always a standard GaN-on-sapphire template, which was included for comparison purposes. The influence of a variety of parameters on misfit-dislocation formation was examined in these studies; these parameters included: (i) $In_xGa_{1-x}N$ composition, which varied from x~0.09 up to x~0.17, (ii) InGaN heterolayer thickness, h, which varied from h~150 nm up to h~600 nm, and (iii) V/III ratio, which was controlled by varying the ammonia flow rate from ~5 slm up to ~15 slm. Following growth, the samples were examined by SEM/CL to image misfit dislocations, by standard SEM and/or AFM to determine surface morphology, and by XRD to determine composition and strain. Many detailed results of these experiments have previously appeared in our monthly reports; here we summarize only the major conclusions of these lengthy experiments.

For the InGaN/GaN heterostructures and growth conditions examined, long-range misfit-dislocation glide at the InGaN/GaN heterointerface was only sporadically observed. Averaging over all experiments, only about one of every four samples showed evidence of long-range misfit-dislocation glide in CL, SEM, or AFM images. In the limited instances where long-range glide was successfully observed, the glide never produced a degree of strain relaxation greater than ~ 15%. Moreover, the occurrence of long-range glide did not appear to depend on the initial threading-dislocation density or the type of GaN template. In fact, all of the different types of GaN templates tried, including our standard GaN templates on sapphire, randomly showed long-range misfit-dislocation glide. Our observations fail to confirm the original hypothesis of the ASU group that the initial threading-dislocation density of the GaN fully controls the relaxation mode. The sporadic results obtained for our larger set of observations instead suggests that an uncontrolled extraneous source may control heterogeneous nucleation of the linear misfit dislocations (for example, stress-concentrating particulates introduced during sample handling, loading, or growth). At present, we are left without a means to control the poorly understood nucleation of these linear misfit dislocations.

Alternative Modes of Strain-Relaxation in InGaN/GaN:

Since the sought-after linear misfit dislocations either fail to appear, or fail to produce a high degree of strain relaxation even if they do appear, the dominant mode of strain relaxation always shifts to other less-desirable mechanisms as the InGaN layer composition and thickness are increased. Broadly speaking, three different relaxation pathways are observed to compete in these heterostructures, and the resulting dominant relaxation behavior depends on the specific InGaN growth conditions.

The first pathway proceeds by "patchy" desorption of portions of the initial InGaN layer during growth, which leads to an initially planar InGaN layer containing a large number of perforations or holes. InGaN tends to regrow with a rough morphology in these holes, and as the process proceeds with increasing film thickness, the surface appears to become entirely converted to roughened InGaN through regrowth in the ever-expanding perforations.

The second pathway centers around v-defects formed at pre-existing threading dislocations or formed above the path of any linear misfit dislocations that sporadically appear in the layers. As the film thickens, stress concentrations at the base of the v-defects punch out localized dislocation loops that expand along the basal plane to surround the base of each v-

defect. These floret-shaped dislocation arrays nucleate further v-defects at the periphery of each initial v-defect; the localized strain relaxation produced by these dislocation arrays simultaneously accelerates the InGaN growth rate in the same region. Both effects combine to increasingly roughening and to relax the heterolayer with increasing thickness.

The third pathway is stress-induced morphological instability of planar InGaN, which takes hold in planar regions of the InGaN layer when the first two mechanisms are less dominant. On a planar growth surface, small, random deviations from planarity tend to occur. If the heterolayer is lattice mismatched, this leads to a well-known stress-induced instability where high spots in layer grow at a different rate from low spots in the layer because of the slight differences in strain energy at each position [Asaro and Tiller, Met. Trans. **3**,1789 (1972)]. This growth-rate instability becomes exponentially amplified with thickness, such that dense arrays of grooves eventually form all across the layer as thickness increases. In compressively strained heterolayers such as InGaN on GaN, stress concentrations at the base of these grooves concomitantly nucleate localized misfit dislocations, in manner similar to that described above for v-defects.

Unfortunately, none of these three observed pathways led to strain-relaxed InGaN with a surface morphology and threading-dislocation density suitable for growing high-IQE InGaN quantum wells. Thus, our experiments to date suggest that Approach 3 under Task 1 is not a suitable method for growth useful strain-relaxed InGaN templates.

Task 1 / Approach 4: Growth of InGaN using compositionally graded heterostructures

This approach was examined during Budget Period 1; minimal further experiments were conducted during the present reporting period.

Task 1 / Approach 5: Growth of InGaN using Sc interlayers

Based on our continuing need to develop an approach to lower threading-dislocation density in our relaxed InGaN successfully grown using AlN interlayers (Task 1 / Approach 1), we investigated a new interlayer growth method that involves the insertion of ScN interlayers into the heterostructure to reduce threading dislocations. While this approach was not explicitly included in our original plan, it represented an extension of our previous Task 1 plans involving AlN and GaN interlayers. ScN interlayers have recently proved very successful for reducing threading dislocations in GaN [M. A. Moram *et al.*, Appl. Phys. Lett. **91**, 152101 (2007)], and we therefore decided to test the applicability of this scheme for our relaxed InGaN layers grown on AlN interlayers.

Scandium metal films were deposited by pulsed-laser deposition on ~3-μm-thick template layers of GaN on sapphire. These Sc films were nitrided in a MOCVD reactor by annealing under NH_3 flow. The effect of pressure, temperature, and time on nitrided-film uniformity was studied. It was found that the film changes from opaque-grey to transparent-yellow color when Sc converts to ScN. Energy-dispersive X-ray (EDS) spectroscopy confirmed that there was no loss of Sc during nitridation. Lower pressures and temperatures were found to yield better film uniformity.

We attempted regrowth of GaN on thick (h > 16 nm) ScN films, using a two-step process: (i) the film was nucleated at reduced temperature (~800-950 ^{o}C, depending on the sample), followed by (ii) 60 minutes of high-temperature (1050 ^{o}C) growth. We observed poorly aligned and separated grains at the center of the wafer, well-aligned grains near the edge, and some regions of coalescence. Uniform coalescence was found to be difficult in our numerous attempts. We also attempted regrowth of GaN on ScN interlayers deposited on thick AlN templates on sapphire. Poorly aligned grains were again observed near the wafer center along with channel-fracture patterns at the wafer edge. GaN nucleation in these AlN crack arrays at the wafer edge led to ELO-like lateral GaN growth, revealing that ScN interlayers basically function as randomly self-patterned "auto-masks" for ELO, much like other thin interlayers reported in the literature (SiN_x, TiN).

We also attempted similar GaN regrowths on thin (h < 6 nm) interlayers. The microstructure of the regrown GaN was more uniform across the wafer surface. The films were fully coalesced, but still not adequately planar.

Reproducing the previously published ScN interlayer results for reducing dislocations in GaN proved to be more difficult than anticipated. As a result, attempts to grow InGaN films on the ScN layers have not been attempted. We may, or may not, continue to explore this approach to attaining strain-relaxed InGaN templates, depending upon the progress that we make in nanopatterned-growth work in Task 2 during the final Budget Period.

The work reported in this section was conducted jointly with another of our EERE funded projects "Novel ScGaN and YGaN Alloys for High Efficiency Light Emitters" (M6642867), Dan Koleske, PI. Further details are given in the final report for that project.

Task 1 / Approach 6: Growth of InGaN on thick AlN templates

Our previous work on Task 1 / Approach 1 showed that thin AlN interlayers efficiently induce strain relaxation, but at the same time, they produce high threading-dislocation densities. One thought is that the rough, three-dimensional morphology of the AlN interlayer plays a key role in generating these threads, but this rough starting surface may not in fact be needed to induce relaxation -- the relaxation may instead result primarily from growth on the more highly lattice-mismatched AlN surface. If this is true, growth on thick, planar AlN templates (instead of on rough AlN interlayers on GaN) might yield a relaxed InGaN layer with a lower threading-dislocation density. To test this idea, we grew strain-relaxed InGaN on thick AlN templates as an extension of our original AlN-interlayer approach. Andrew Allerman, our growth specialist for AlGaN/AlN materials, was tasked with providing the AlN/SiC or AlN/sapphire templates needed for these experiments.

We grew 2-μm-thick AlN layers on SiC substrates and diced these wafers into quarter-wafer pieces, upon which we grew two different strain-relaxed InGaN/GaN heterostructures. Both structures consisted of a 10-period InGaN/GaN superlattice with a period of 38.0 nm and an InGaN/GaN thickness ratio of ~10:1 (x=0.057 for the first sample and x=0.110 for the second sample).

X-ray diffraction (XRD) was used to characterize the two strain-relaxed InGaN/GaN heterostructures grown on AlN/SiC. XRD found the expected InGaN compositions

(x=0.057 and x=0.115) and a degree of strain relaxation in the 65-100% range, which is similar to the degree of relaxation we previously observed for growth on AlN interlayers. InGaN peakwidths were also similar to or exceeded those of similar structures grown on GaN using AlN interlayers. The broad peakwidths suggested that InGaN growth on thick AlN will not provide a viable route to reduced threading-dislocation density.

Task 2: Epitaxial lateral overgrowth of strain-relaxed InGaN using FACELO

We began our studies on the FACELO approach by growing ELO GaN pyramidal stripes at 950 ºC. The pyramidal bases were 3.8 micron wide, with the base of adjacent stripes separated by just 0.2 microns. We then grew a 30-nm-thick AlN interlayer on the stripes, followed by 360-nm-thick InGaN of composition x=0.05. The purpose was to examine the strain relaxation, defectivity, and surface morphology produced when we perform InGaN FACELO on the {11-22} facets of GaN.

During post-growth characterization, the overgrown InGaN composition was found to be x=0.046, and the wafer had a smooth and specular appearance and no evidence of grey discoloration. The InGaN strain-relaxation was 59%, similar to that found for InGaN growth on unpatterned GaN templates on sapphire. We also found a reduction in the XRD symmetric (0002) peakwidth suggesting a modest decrease in threading density compared to planar growth; the extent of the reduction was not well quantified due to uncertain interpretation of peakwidths for InGaN growths conducted on the faceted stripes.

To explore facet evolution with film increasing thickness, we performed an additional regrowth on this FACELO sample (the "first regrowth"). The next regrown layer was a 5-period, 500-nm thick, x=0.075 superlattice (the "second regrowth"). The GaN portion of the superlattice was grown at 985 ºC; InGaN portions were grown at 838 ºC to maintain average superlattice composition near x=0.05. For both regrowths, SEM analysis showed formation of a basal plane at the top of the pyramidal facets, but not at the bottom of the trough. For the second regrowth, XRD analysis of the In composition suggested that In did not appreciably incorporate on the sloped {11-22} facets during the regrowth. Instead, lateral growth of the facets mainly occurred due to GaN deposition only.

A separate FACELO experiment was done in which the entire structure was grown in a single run without interrupts for inspection. An $In_{0.05}Ga_{0.95}N$ single-heterolayer was grown as a continuous alloy to a total thickness of 860 nm -- without using the InGaN/GaN superlattice approach deployed for the uppermost part of the previous sample. The goal was to compare the two samples and determine how surface-facet formation and indium incorporation are influenced by continuous growth versus superlattice growth. We observed little development of a c-plane facet at the top of the GaN pyramids, and infer that the continuously grown InGaN is conformal to the underlying pyramidal GaN stripes.

There is an anisotropic in-plane strain distribution that arises because the pyramidal stripes produce different InGaN strain-relaxation along directions parallel and perpendicular to the stripe. The inclined facet modifies the elasticity theory needed for a rigorously correct interpretation of the x-ray data. The asymmetric (20-25) reflection was used to examine in-plane strain parallel to the stripe and the asymmetric (11-24) reflection was used for strain perpendicular to the stripe. We found very different strains and compositions parallel and

perpendicular to the stripe confirming the hypothesized anisotropic in-plane strain. The InGaN strain parallel to the stripe is mostly unrelaxed while strain perpendicular to the stripe is substantially relaxed.

In further XRD studies of this second sample, the InGaN regrown on the basal plane located at the apex of the GaN pyramidal stripes was found to be untilted in orientation, with an approximate composition x~0.050 and a strain relaxation near 65%. In contrast, InGaN regrown on the center of the {11-22} sidewall facets exhibited a tilted InGaN orientation, with an approximate composition x~0.024 and a strain relaxation near 50 %. The facet composition was reduced by a factor of two relative to the basal plane, in agreement with trends previously observed by others where indium incorporation is reduced for higher composition quantum wells also simultaneously grown on {11-22} and {0001} facets [see, for example, Nishizuka *et al.*, APL **85**, 3122 (2004)]. A subsequent SEM/EDS analysis gave an In fraction x~0.050 at the tops of the stripes and x~0.030 on the sidewall facets, in good agreement with our XRD analysis.

A similar SEM/EDS analysis of the first FACELO sample (in which the superlattice structure described before was grown) showed the clear presence of aluminum at the top centerline region of the stripe. The fact that the AlN interlayer remains observable by EDS after subsequent InGaN and GaN regrowths supports the notion that minimal basal plane deposition has occurred during these regrowths – material was instead predominately incorporated on the {11-22} facets to produce mainly lateral extension of the basal plane facet.

Due to the tendency for strongly reduced In-composition on the inclined facet and the observed conformal growth for the InGaN (which limits the prospects for planarization at the few-micron length scale), the FACELO approach to achieving strain-relaxed InGaN templates does not appear promising. Thus, our emphasis in Task 2 turned to a nanopatterning approach, described next.

Task 2: Dislocation reduction using nanopatterned growth of strain-relaxed InGaN

Nanolithography Process Development

Prof. Steve Brueck at the University of New Mexico (UNM) maintains an interferometric lithography (IL) laboratory capable of producing 1D stripe arrays or 2D dot arrays with critical dimensions of ~200 nm or less. To gain quick and less costly access to a large-area nanopatterning capability, we initiated a contract to UNM to obtain user access to their facility to use their IL laboratory to apply, expose, and develop nanopatterns in photoresist films, as needed to produce nanopatterned GaN to be used for subsequent regrowths of patterned, strain-relaxed InGaN. Most other supporting processes including dielectric thin-film deposition, metal thin-film deposition, metal liftoff, plasma etching, and wet etching were carried out at Sandia's MESA MicroFab cleanroom facility. This mix of processing venues allowed us to take advantage of both UNM's unique IL nanopatterning laboratory and Sandia's superior processing facilities for compound semiconductors. In particular, we minimized process-development efforts by leveraging the technical expertise, the standard processes, and the better process stability available in the Sandia MicroFab.

For the nanopatterning experiments described below we used 2-μm-thick GaN templates grown on sapphire. A plasma-enhanced chemical-vapor-deposition (PECVD) tool located within the MicroFab was used to subsequently deposit a 50-nm-thick SiO_2 layer. Lithography was performed using a 355-nm-wavelenth frequency tripled Nd:YAG laser. Prior to laser-interferometric exposure, a 120-nm-thick antireflective coating (Brewer Science i-CON-16) and a 500-nm-thick positive PR film (Shipley SPR505-A) were spin-deposited on the wafers and soft baked.

Reactive-Ion-Etching Process Development

Once exposed by IL and developed, these samples were used to develop multi-step reactive-ion-etching (RIE) procedures for transferring the PR nanopattern onto the underlying ARC, SiO_2, and GaN layers. Our initial process-development efforts successfully yielded GaN nanostripes with a 500-nm pitch, a GaN stripe width of 220 nm, and a trench depth up to 250 nm. However, one challenge was the slope of the stripe sidewalls away from vertical, which produced narrowing of the trenches with increasing depth. We found that further optimization of the ICP process, conducted using 50 W of plasma rf-power and an altered sample bias, yielded nearly vertical sidewalls in the upper half of the channel, but the bottom of the channel still tapered to an undesirable point.

Facet-Selective Wet-Etching Process Development

To remove the remaining sidewall taper, we performed experiments using a facet-selective wet-etching process recently developed in a separate program. This facet-selective etch has a very slow etch rate for {10-10} surfaces and a fast etch rate for most other surface orientations. This anisotropy allowed rapid removal of sloping sidewall materials resulting in vertical {10-10} sidewall surfaces. Since the sidewall planes here were actually along {11-20}, the sidewalls ended-up consisting of microfacets paralleling {10-10} such that the sidewall surface became microfaceted due to the selective wet etch. Nonetheless, the selective etch progressively reshaped and improved the bottom half of the channel, eventually producing straight and vertical sidewalls and a relatively flat-bottomed channel. At room temperature this process took ~110 minutes; heating the etchant to 50 °C reduced the required time to ~30 minutes.

These combined improvements to the ICP and wet etching yield more ideally shaped, high-aspect ratio GaN nanostripes that were well suited to our InGaN growth studies.

InGaN Growth Studies on Nanopatterned Stripe Arrays

We began our study of MOCVD regrowth of InGaN on top of our initial, less-optimized, GaN nanostripe arrays (from the RIE work, described above). Our first regrowth of $In_{0.1}Ga_{0.9}N$ to a nominal thickness of 150 nm on a GaN nanostripe array produced InGaN stripes with a trapezoidal cross-sectional shape, as expected for the low growth temperature (~810 ºC) required to incorporate indium at x=0.10. Surprisingly little InGaN appeared to grow on the nanostripe sidewalls or at the bottom of the trenches formed by the sidewalls. Some limited lateral growth of the InGaN occurred at the top of the GaN stripes, and the resulting InGaN-stripe thickness and width was just short of the initial coalescence point for adjacent stripes.

A preliminary analysis of x-ray diffraction data for this InGaN/GaN nanostripe array indicated that the InGaN stripes had a composition near to the expected value of x=0.10 obtained from separate calibrations. Moreover, the InGaN stripes appeared to be unrelaxed parallel to the stripe direction and partially relaxed perpendicular to the stripe direction, just as we expected for elastic deformation of the InGaN/GaN couple due to the high-aspect-ratio geometry of the nanostripe. Fully quantitative results for the XRD analysis of composition and strain will require the development of elasticity theory that takes into account the non-biaxial strains produced in the InGaN by the anisotropic stripe geometry. Development of the needed theory will continue in the next Budget Period.

The focus of continuing efforts to grow nanopatterned-InGaN will be twofold: (i) to investigate the effect of growth parameters on the InGaN facet geometry, and (ii) to grow thicker InGaN films that achieve coalescence. These experiments will also put to use our newly improved facet-selective wet-etching process.

Task 3: Growth of high-indium-composition active regions on strain-relaxed InGaN

In this Budget Period we continued efforts to grow and characterize InGaN/GaN multiple quantum well (MQW) active regions on top of strain-relaxed InGaN templates (x=0.037 and x=0.103 strain-relaxed InGaN/GaN superlattice templates). For this work, we reduced the number of MQW layers to 4 (from the previously used 10) in an effort to eliminate the extreme v-defect formation seen earlier. We also somewhat altered the InGaN regrowth layer immediately below the MQWs, using a 100-nm, x=0.02 layer, and increasing the buffer growth temperature to 880 ºC to avoid v-defect formation in this buffer layer. The rms surface roughness of the MQWs was in the 3-to-5 nm range, much better than the 14 nm seen for the 10-MQW samples. However, improved roughness approaching the 1-nm range is ultimately needed.

For these MQW samples on strain-relaxed InGaN templates, redshifts of 17-39 nm were observed, perhaps due to the lower baseline composition in the QW. The general trend reconfirms the trend previously found in Budget Period 1: the nominal increase in the QW composition produced by use of a strain-relaxed InGaN template roughly equals the In-composition of the underlying strain-relaxed InGaN template.

Task 4: Development of p-type materials, heterostructures and thermal-activation processes

Our work on Task 4 focused on improving the hole concentration in p-type InGaN films. These experiments involved 14 separate MOCVD growth runs composing a parametric study that investigated the influence of variations in both the NH_3 flow rate and the Mg-precursor flow rate. After each growth run, the hole concentration was determined using Hall-effect measurements conducted at 5 different positions on each wafer. Optical-reflectance measurements made both before and after InGaN growth were used to accurately determine InGaN film thicknesses needed for accurate determination of hole concentrations by Hall effect. X-ray diffraction was used to measure the indium concentration and verify the InGaN strain state.

For these optimization studies, the InGaN growth rate was ~200 nm/hour and the InGaN growth temperature was 820 °C. In studies varying the NH_3 flow rate from 7 to 15 slm, an NH_3 flow rate of 15 slm combined with an N_2 flow 10 slm was found to produce the best incorporation of indium into the InGaN. XRD measurements found that the resulting indium concentrations ranged from 7 to 8%, and the InGaN was found to be coherently strained to the underlying GaN, as intended. The optimized NH_3 and N_2 flow conditions differ from those used in our earlier p-doping work (NETL monthly report, 5/15/07) where lower NH_3 flows were used.

Following optimization of the NH_3 flow rate, the flow rate of the Mg precursor (bis-cyclopentadienylmagnesium or cp_2Mg) was coarsely varied from 40 to 120 sccm, with the highest hole concentration occurring near 80 sccm. We conducted more detailed experiments examining the effect of varying the Mg-precursor flow rate in a narrower range around 80 sccm. The average measured hole concentration and mobility were examined as a function of the Mg-precursor flow rate. The data confirmed 80 sccm as the optimum Mg-precursor flow rate, and at this flow rate, the average hole concentration maximized at ~$3.0x10^{18}$ cm^{-3}, with individual hole concentrations ranging from $2.1x10^{18}$ cm^{-3} to $4.4x10^{18}$ cm^{-3} at various positions on the wafer. These average and maximum hole concentrations meet or exceed all p-type doping levels targeted in our milestones and also far exceed our initial results reported in May, 2007. The improved results here may be due to both the differently optimized InGaN growth conditions now in use and the use of InGaN with higher indium composition.

6. Status of Milestones

Each task listed in Section 4 has various milestones that have become due during either Budget Period 2 or the last three months of Budget Period 1. For reference, Table II -- located at the end of this section -- shows our project's milestones after their revision in mid-2007. Below, we summarize progress towards these milestones attained in the last 15 months.

Task 1 / Month-27 Milestone on planar heteroepitaxy:

Over the course of Budget Periods 1 and 2, numerous strain-relaxed InGaN templates have been produced or attempted using the various planar-growth approaches and strategies outlined in our original project proposal. As reported in our early Budget-Period 1 work (see September-2006 report), we have obtained highly relaxed $In_xGa_{1-x}N$ with compositions in the range $0.05<x<0.40$, but rough surface morphology and high threading-dislocation densities limit suitability of these relaxed materials for subsequent active-region growth. For compositions $x<0.12$, the combined use of multiple InGaN growth strategies developed under Task 1 (AlN interlayers, GaN planarization layers, and compositional grading) yielded significant improvements to surface morphology such that quantum-well active regions were successfully grown on these templates (see March- and April-2007 reports, and May-2008 report). However, threading-dislocation densities remain unacceptably high, and our other planar-growth strategies fail to produce needed reductions in threading density. **Consequently, we consider this milestone largely complete but only partially successful.**

To obtain further required reductions in threading-dislocation density, we plan to rely on nanopatterned growth methods currently being developed under Task 2, with minimal further work currently planned under Task 1.

Task 2 / Month-15 Milestones on micron-scale ELO / FACELO:

Work towards these two closely related milestones was summarized in four monthly reports dated July to October of 2007. The work that was performed emphasized FACELO type growths where InGaN was grown on patterned and facetted GaN stripes, and, only a few selected attempts at true ELO of InGaN were performed. During the FACELO experiments, InGaN growth on the {11-22} facets of GaN showed significantly reduced indium incorporation relative to blanket growth on (0001) surfaces. Moreover, it proved difficult to promote c-plane facet development at the bottom of the stripe trenches during attempted lateral growth of InGaN on adjacent GaN facets. The main lesson learned was that a pattern design that allows InGaN growth to proceed on c-plane facets from the very start might be preferred. Our ongoing nanopatterning work will therefore initially focus on pattern architectures that rely on basal plane growth.

A second major lesson regarding micron-scale patterned growth of InGaN comes from our extensive work in Task 1 to develop planar growth of InGaN. A clear outcome of these planar growth experiments is that it is extremely difficult to maintain high-quality InGaN growth for film thicknesses beyond about 200-500 nm for $In_xGa_{1-x}N$ alloys with the compositions sought in our project ($0.08 < x < 0.16$). Greater thicknesses typically lead to degradation of the InGaN film morphology through stress-induced surface instabilities, which are difficult to suppress. This limitation on InGaN film thickness fundamentally limits micron-scale ELO of InGaN in two important ways: (i) it prevents one from reaching the film thickness required to laterally coalesce micron-scale patterns, and (ii) because the thickness of the InGaN remains much less than the few-micron-wide lateral surfaces on which growth occurs, the patterning has limited influence on the evolution of the InGaN epilayer -- because locally, the growth remains essentially planar in character.

Because of the limitations revealed by these studies, we regard the work on micron-scale ELO/FACELO of InGaN to be completed, as further work is unlikely to produce the needed reduction of threading dislocations in strain-relaxed InGaN. **Thus, we consider the two Month-15 Milestones of Task 2 to be complete.**

Task 2 / Month-21 Milestone on process-development for nanopatterned InGaN growth:

The purpose of the nanopatterning approach is to reduce the patterning dimensions used in the above ELO/FACELO growth experiments by about 10-fold -- from the few-micron scale down to the few-100-nm scale. This makes the usable InGaN film thicknesses (~200-500 nm) comparable to the nanopattern feature sizes. This similarity in dimensions should enable a useful, three-dimensional elastic and plastic response for strained InGaN growth on nanopatterned GaN -- such a response is not possible when few-hundred-nm-thick InGaN layers are grown on micron-scale patterns, as discussed above.

Month-21 of our project corresponds to roughly April of 2008. Due to an intense focus on Task 1 on planar heteroepitaxy during the middle part of FY08, we did not start work on this

nanopatterning milestone until May of 2008. Since that time, progress has been good, as can be seen in our four monthly reports dated May to August of 2008. More recently, we have developed processes yielding our first, broad-area, nanopatterned GaN templates, and we have conducted successful first growths of partially strain-relaxed InGaN on top of these GaN nanostripe arrays. **These last two events mark successful, but late completion of the Month-21 Milestone of Task 2 to develop an initial nanoscale-patterning capabilities and to extend patterned InGaN growth experiments to the submicron feature sizes.**

Task 2 / Month-27 Milestone on refinement of nanopatterned InGaN growth:

Due to the delayed start of the preceding milestone, experiments to further refine our processing and growth capabilities for producing nanopatterned InGaN/GaN materials also began late -- at the very end of Budget Period 2. **This milestone thus remains incomplete.** We are currently working to shift our nanopatterning process from fabrication of 1-D nanostripe arrays to more challenging 2-D nanopost arrays. We aim to complete this nanopatterning development work within the first 3 months of our final Budget Period.

Task 3 / Month-27 Milestone on InGaN active-region growth on relaxed InGaN:

During Budget Period 1 (see June-2007 report), we first reported InGaN/GaN quantum-well active regions regrown on strain-relaxed InGaN, where the quantum wells emitted at ~531 nm. **Because of these results, we attained early completion of our Budget-Period 2 Milestone under Task 3.** Nonetheless, we anticipate further active-region development work during our final Budget Period, as work progresses on our strain-relaxed InGaN templates.

Task 4 / Month-27 and Month-39 Milestones on p-doping of InGaN:

As discussed in our September-2008 monthly report, we successfully improved the hole concentration in our p-type InGaN films by performing a parametric study of MOCVD growth that investigated the influence of variations in both the NH_3 flow rate and the Mg-precursor flow rate. These recent optimization studies proved more successful than our earlier doping studies, and we achieved individual hole concentrations ranging from 2.1×10^{18} cm^{-3} to 4.4×10^{18} cm^{-3} at various positions on selected wafers. **Thus, we have completed our Month-27 milestone on p-type doping on schedule, and we have also completed our Month-39 milestone on p-type doping well ahead of schedule.**

Task 5 / Month-27 Milestone on IQE evaluation:

Work on this milestone has yet to begin because the threading-dislocation density of our existing strain-relaxed InGaN templates remains much too high to merit investment in IQE evaluations. **This milestone therefore remains incomplete.** The most pressing goal of ongoing work is to reduce threading-dislocation densities in our strain-relaxed InGaN such that plausible attempts to demonstrate improved IQE can begin.

Table II. Revised project milestones as of July 2007. The items shown in red are the revisions or additions made to the original project milestones dating from the project start in July 2006.

Task 1 -- Planar heteroepitaxy of strain-relaxed InGaN/GaN templates		
Month 12 Milestone	Month 27 Milestone	
Produce strain-relaxed $In_xGa_{1-x}N$ templates with x=0.08 that are suitable for active-region materials growth	Produce compositionally graded, strain-relaxed $In_xGa_{1-x}N$ templates with x=0.16 that are suitable for active-region growth	
Task 2 -- Epitaxial lateral overgrowth of strain-relaxed InGaN Templates		
Month 12 Milestone	Month 21 Milestone	Month-39 Milestone
Perform initial experiments to determine mask selectivity for InGaN alloys grown by traditional micron-scale ELO (The reduced scope reflects our incomplete progress on this milestone to date.)	Complete initial development of nanoscale patterning capability and extend InGaN ELO/FACELO experiments to growth on nano-patterned materials with a period of < 500 nm.	Develop further improvements in surface morphology and threading-dislocation density. Produce strain-relaxed ELO $In_xGa_{1-x}N$ templates with x=0.16
Month 15 Milestone	Month 27 Milestone	
Perform experiments to evaluate growth anisotropy, facet evolution, strain-relaxation, and composition for InGaN alloys grown by traditional micron-scale ELO	Refine nanopatterning capabilities and optimize MOCVD growth conditions to produce strain-relaxed ELO $In_xGa_{1-x}N$ templates with x=0.08	
Month 15 Milestone		
Perform experiments to evaluate strain-relaxation, composition, morphology and dislocation density in InGaN alloys grown on faceted GaN by micron-scale FACELO		
Task 3 -- Growth of high-indium-composition active regions on strain-relaxed InGaN		
Month 12 Milestones	Month 27 Milestone	Month 39 Milestone
Produce $In_xGa_{1-x}N$ active regions on relaxed InGaN with: x~0.21 in the well, λ=505 nm	Produce $In_xGa_{1-x}N$ active regions on relaxed InGaN with: x~0.23 in the well, λ=525 nm	Produce $In_xGa_{1-x}N$ active regions on relaxed InGaN with: x~0.25 in the well, λ=545 nm
Task 4 --Development of p-type materials, heterostructures and thermal-activation processes		
	Month 27 Milestone	Month 39 Milestone
	Demonstrate p-$In_xGa_{1-x}N$ with $p \geq 1.5 \times 10^{18} cm^{-3}$ for a composition in the range x=0.05-0.20	Demonstrate p-$In_xGa_{1-x}N$ with $p \geq 3 \times 10^{18} cm^{-3}$ for a composition in the range x=0.05-0.20
Task 5 -- Evaluation of the internal quantum efficiency of deep-green emitters		
	Month 27 Milestone	Month 39 Milestone
	Demonstrate p-n junction EL with: λ=525 nm, IQE=15% (75 lm/W per Attachment A)	Demonstrate p-n junction EL with: λ=545 nm, IQE=25% (150 lm/W per Attachment A)

7. Cooper Stage-Gate Progress

Our program is in the Stage 2 ("Applied Research") category according to the Cooper Stage-Gate process and will likely remain in this stage throughout this program. If progress through the project is successful, then information gained in this program could be transferred to Stage 3 "Exploratory Development" or Stage 4 "Advanced Development".

8. Deliverables

We will document the findings of our research in a final report submitted to the DOE Project Manager. The following topics will be covered:

- Task 1: Planar Heteroepitaxy of Strain-Relaxed InGaN/GaN Templates
- Task 2: Epitaxial Lateral Overgrowth of Strain-Relaxed InGaN Templates
- Task 3: Growth of High-Indium-Composition Active Regions on Strain-Relaxed InGaN
- Task 4: Development of p-type Materials, Heterostructures, and Thermal-Activation Processes
- Task 5: Evaluation of the Internal Quantum Efficiency of Deep-Green Emitters

The final report will give detailed descriptions of the activities, results, and implications for Solid-State Lighting in each of the tasks. We will also submit to the DOE Project Manager annual technical reports and Monthly Highlight Communications of developments, achievements, changes, and problems, meeting the specific guidelines set forth by DOE / NETL.

9. Final Product / Commercialization

The overall goal of our project is to improve material quality and luminescence efficiency in high-indium-content InGaN. This would be a core technology improvement that would impact a very broad cross-section of industrial III-Nitride epitaxial material producers.

We will contribute to the rapid success of Solid-State Lighting by transferring our applied research findings to Solid-State Lighting Industrial Product Development members (SSL Partnership and SSL Industry members) by the mechanisms outlined in Section II, Part 7 (Exceptional Circumstances) of the Call for Proposals.

Our licensing strategy includes aggressively seeking patents of the intellectual property arising from this research. Such protection of the IP makes it more attractive to industry for licensing and use in commercial products. Sandia has an Intellectual Property Center devoted to patenting and licensing our technology. We have a good track record in licensing our compound semiconductor technologies to companies, e.g., vertical-cavity surface-emitting laser (VCSEL) patents, *in situ* growth rate monitor, *in situ* stress monitor, and Chemkin software. In addition, we have applied for 2 U.S. patents and have filed another 12 patent disclosures as a result of our concluded Grand Challenge LDRD project on solid-state white lighting.

Sandia can negotiate exclusive or non-exclusive license agreements for its IP (depending upon needs of our partners and other restrictions, such as the Determination described on pages 14 and 15 of the Call for Proposals). A potential barrier that could arise would be if more than one company should desire to obtain exclusive license to this technology. We will engage in good-faith negotiation with all potential licensees and will also be guided by rules of the modified intellectual property arrangements of the Determination.